

J/ψ absorption by π and ρ mesons in meson exchange model with anomalous parity interactions

Yongseok Oh,^{*} Taesoo Song,[†] and Su Hounng Lee[‡]

*Institute of Physics and Applied Physics and Department of Physics, Yonsei University, Seoul
120-749, Korea*

Abstract

We reanalyze the dissociation process of the J/ψ by π and ρ mesons into $D + \bar{D}$, $D^* + \bar{D}$, $D + \bar{D}^*$, and $D^* + \bar{D}^*$ within a meson exchange model. In addition to the dissociation mechanisms considered in the literature, we consider anomalous parity interactions, whose couplings are constrained by heavy quark spin symmetry and phenomenology. This opens new dissociation channels and adds new diagrams in the previously considered processes. Compared to the previous results, we find that these new additions have only a minor effect on the $\rho + J/\psi$ total inelastic cross section, but reduce the one for $\pi + J/\psi$ by about 50 % near the threshold.

PACS number(s): 25.75.-q, 12.39.Fe, 12.39.Hg, 13.75.-n

Typeset using REVTeX

^{*}Email address: yoh@phya.yonsei.ac.kr

[†]Email address: tssong@phya.yonsei.ac.kr

[‡]Email address: suhounng@phya.yonsei.ac.kr

I. INTRODUCTION

Suppression of J/ψ production is considered to be one of the promising signals for detecting the formation of the quark-gluon plasma (QGP) in relativistic heavy ion collisions (RHIC) [1,2]. Indeed, recent reports by the NA50 Collaboration [3,4] show an anomalous suppression of J/ψ production in Pb+Pb collisions at CERN. Model calculations, which assume the formation of a deconfined state of quarks and gluons [5,6] at the initial stages of the collision, seem to be successful in explaining the anomalous suppression. However, before coming to a definite conclusion on the existence of the QGP state in such collisions, it is essential to investigate whether the observed J/ψ suppression can be explained by a more conventional approach that does not assume the existence of QGP state. In such models, the suppression comes from the absorption of J/ψ by the co-moving hadrons [7–10]. Since such co-mover models strongly depend on the cross sections of J/ψ absorption by hadrons, it is essential to have a better knowledge of the magnitude and energy dependence of the cross sections. This is not an easy task, but is indispensable for true identification of QGP in RHIC.

The absorption of J/ψ by light hadrons has been investigated using various methods [11–18]. The estimated values for the cross sections show a strong dependence on the hadronic models and assumptions on the absorption mechanisms employed in the calculation. The first set of models uses the quark degrees of freedom. Using perturbative QCD in the heavy charm quark mass limit [19], Kharzeev, Satz, and their collaborators [11,12] found very small absorption cross sections at the order of μb . In Ref. [13], Martins, Blaschke, and Quack investigated the charmonium dissociation processes, $\pi + J/\psi \rightarrow D^* + \bar{D}$, $D + \bar{D}^*$, and $D^* + \bar{D}^*$ using quark exchange model and found a strong enhancement near the threshold with an exponential falloff at higher energies. The peak was found at $\sqrt{s} \simeq 4$ GeV with a value of about 7 mb. This calculation was recently improved by Wong, Swanson, and Barnes [14] by using a more successful quark-interchange model and hadron wave functions. The cross section for $\pi + J/\psi$ was found to be relatively small with a maximum of about 1 mb, while the pion induced ψ' dissociation process had a much larger cross section with lower threshold for the initial kinetic energy.

Another approach to J/ψ absorption is to use effective meson Lagrangian [15–18]. In this approach, the authors considered t -channel meson exchanges to estimate the J/ψ absorption cross sections. In Ref. [15], Matinyan and Müller calculated D meson exchange diagrams and found small cross sections around 0.3 mb for $\pi + J/\psi$ and $\rho + J/\psi$. The obtained cross sections were found to increase with energy. This calculation was improved by Haglin [16], who included D^* meson exchanges and four-point couplings in the J/ψ absorption mechanisms. Similar calculations were recently performed by Lin and Ko [17]. The new results show a rather large cross section for $\pi + J/\psi \rightarrow D^* + \bar{D}$ and $D + \bar{D}^*$, i.e., about 20 mb at $\sqrt{s} = 4$ GeV, which at higher energies saturates to about 30 mb.¹ However, for a realistic structure of the mesons, form factors have to be taken into account. Inclusion

¹The typo errors in Ref. [16] and different conventions between Refs. [16,17] are cleared recently by Ref. [18].

of form factors generally reduces the cross sections. With suitable form factors and cutoff parameters, which however cannot be justified *a priori*, Lin and Ko [17] concluded that the saturated absorption cross sections for $\pi + J/\psi$ and $\rho + J/\psi$ are around 7 mb and 3 mb, respectively.

All of the meson exchange model calculations discussed above essentially use the same effective meson Lagrangian; namely the minimal SU(4) Yang-Mills Lagrangian. Two immediate questions can arise. The first is the use of SU(4) symmetry in constructing the effective Lagrangian. Obviously, charm quark is much heavier than the other three light quarks and the SU(4) symmetry is nowhere near being true in QCD. Nevertheless, the starting point of using the SU(4) Lagrangian is to categorize the possible interaction vertices among the meson multiplets and estimate as many of their respective couplings by phenomenology as possible. Doing so, not all of the couplings can be fixed. However, it turned out that for couplings that can be checked, one finds that the SU(4) symmetry relations for coupling constants are not totally meaningless [17,18]. Such checks provide the order of uncertainty for the calculated absorption cross sections within the effective Lagrangian method, and makes the calculation meaningful. The second question is whether all possible interactions are considered. It is to this question that we want to address in this paper. The previous studies did not fully take into account all possible set of interaction Lagrangian involving D and D^* . In fact, the anomalous parity interactions which are connected to the gauged Wess-Zumino action are all missing. Furthermore, the anomalous term such as $D^*D^*\pi$ is essential and required by heavy quark spin symmetry and its coupling is strongly constrained to the $D^*D\pi$ coupling [20,21]. As we shall see, inclusion of $D^*D^*\pi$ coupling opens new absorption channels and mechanisms which were not considered in the literature. Therefore, to fully estimate the J/ψ absorption cross section within the hadronic model, it is necessary and important to see the effect of the anomalous interactions to such processes, which we will investigate in this work.

This paper is organized as follows. In Sec. II, we introduce our effective Lagrangian. The interaction Lagrangian needed for J/ψ absorption processes by π and ρ mesons are obtained and the cross sections are evaluated. Then in Sec. III, we determine the coupling constants and give the numerical results for the cross sections. Section IV contains summary and discussions. Some details on deriving our effective Lagrangian are given in Appendix.

II. EFFECTIVE LAGRANGIAN FOR J/ψ ABSORPTION

In the heavy quark mass limit ($m_Q \rightarrow \infty$), effective Lagrangian for light ($\bar{q}q$) and heavy ($\bar{q}Q$ or $\bar{Q}q$) mesons can be constructed to preserve chiral and heavy quark symmetries [20–24]. When the heavy quark flavor is the charm, finite mass corrections are expected to be important and should be introduced in the effective Lagrangian in a systematic way. The couplings of the finite mass corrections can be fixed by “velocity reparameterization invariance” [25] or by phenomenology. This “top-down” approach seems to be most plausible way to construct the effective Lagrangian. However, it is not yet clear how to implement heavy quark symmetry to the interactions of quarkonia with light hadrons as the quarkonium states ($\bar{Q}Q$) such as the J/ψ contain two heavy constituents.

Another approach which was used in previous investigations [15–18] is the “bottom-up”

approach. In this approach, one starts with the SU(4) symmetric chiral Lagrangian. The heavy charm quark mass is then assumed to be taken into account through appropriate symmetry breaking terms [26]. However, since the SU(4) symmetry is badly broken, finding all the appropriate symmetry breaking terms is very hard and beyond the scope of this work. In this paper, therefore, we use the ‘‘bottom-up’’ approach phenomenologically to categorize all the possible interaction vertices among the meson multiplets. The couplings are then determined by experimental data and by implementing heavy quark spin symmetry. Doing so, most of the three point couplings can be determined. For the four point couplings and some three point couplings, where such determination is not possible, we will partly rely on the SU(4) relations as well as other model predictions.

As in Refs. [16–18], we start with the SU(4) Lagrangian for the pseudoscalar mesons and introduce the vector and axial-vector mesons by the massive Yang-Mills approach [27]. The axial-vector fields can be gauged-away as in Ref. [28]. The procedure to obtain the effective Lagrangian is well explained, e.g., in Refs. [17,18] and is summarized in Appendix. The effective Lagrangian for π , ρ , D , and D^* then reads

$$\mathcal{L}_{D^*D\pi} = ig_{D^*D\pi} (D_\mu^* \partial^\mu \pi \bar{D} - D \partial^\mu \pi \bar{D}_\mu^*), \quad (1a)$$

$$\mathcal{L}_{\psi DD} = ig_{\psi DD} \psi_\mu (\partial^\mu D \bar{D} - D \partial^\mu \bar{D}), \quad (1b)$$

$$\begin{aligned} \mathcal{L}_{\psi D^* D^*} = & -ig_{\psi D^* D^*} \left\{ \psi^\mu (\partial_\mu D^{*\nu} \bar{D}_\nu^* - D^{*\nu} \partial_\mu \bar{D}_\nu^*) + (\partial_\mu \psi_\nu D^{*\nu} - \psi_\nu \partial_\mu D^{*\nu}) \bar{D}^{*\mu} \right. \\ & \left. + D^{*\mu} (\psi^\nu \partial_\mu \bar{D}_\nu^* - \partial_\mu \psi_\nu \bar{D}^{*\nu}) \right\}, \end{aligned} \quad (1c)$$

$$\mathcal{L}_{\psi D^* D \pi} = g_{\psi D^* D \pi} \psi^\mu (D \pi \bar{D}_\mu^* + D_\mu^* \pi \bar{D}), \quad (1d)$$

$$\mathcal{L}_{DD\rho} = ig_{DD\rho} (D \rho^\mu \partial_\mu \bar{D} - \partial_\mu D \rho^\mu \bar{D}), \quad (1e)$$

$$\begin{aligned} \mathcal{L}_{D^* D^* \rho} = & ig_{D^* D^* \rho} \left\{ \partial_\mu D_\nu^* \rho^\mu \bar{D}^{*\nu} - D_\nu^* \rho_\mu \partial^\mu \bar{D}^{*\nu} + (D^{*\nu} \partial_\mu \rho_\nu - \partial_\mu D_\nu^* \rho^\nu) \bar{D}^{*\mu} \right. \\ & \left. + D^{*\mu} (\rho^\nu \partial_\mu \bar{D}_\nu^* - \partial_\mu \rho_\nu \bar{D}^{*\nu}) \right\}, \end{aligned} \quad (1f)$$

$$\mathcal{L}_{\psi DD\rho} = -g_{\psi DD\rho} \psi^\mu D \rho_\mu \bar{D}, \quad (1g)$$

$$\mathcal{L}_{\psi D^* D^* \rho} = g_{\psi D^* D^* \rho} \psi_\mu (2D^{*\nu} \rho^\mu \bar{D}_\nu^* - D^{*\nu} \rho_\nu \bar{D}^{*\mu} - D^{*\mu} \rho^\nu \bar{D}_\nu^*), \quad (1h)$$

where $\pi = \boldsymbol{\tau} \cdot \boldsymbol{\pi}$, $\rho = \boldsymbol{\tau} \cdot \boldsymbol{\rho}$, and we define the charm meson iso-doublets as

$$\begin{aligned} \bar{D}^T &= (\bar{D}^0, D^-), & D &= (D^0, D^+), \\ \bar{D}^{*T} &= (\bar{D}^{*0}, D^{*-}), & D^* &= (D^{*0}, D^{*+}). \end{aligned} \quad (2)$$

In addition to the normal terms given above which were used by Refs. [16–18], there are anomalous parity terms. The anomalous parity interactions with vector fields can be described in terms of the gauged Wess-Zumino action [29] and are summarized in Appendix. By the same method used to obtain the normal terms, we get

$$\mathcal{L}_{D^* D^* \pi} = -g_{D^* D^* \pi} \varepsilon^{\mu\nu\alpha\beta} \partial_\mu D_\nu^* \pi \partial_\alpha \bar{D}_\beta^*, \quad (3a)$$

$$\mathcal{L}_{\psi D^* D} = -g_{\psi D^* D} \varepsilon^{\mu\nu\alpha\beta} \partial_\mu \psi_\nu (\partial_\alpha D_\beta^* \bar{D} + D \partial_\alpha \bar{D}_\beta^*), \quad (3b)$$

$$\mathcal{L}_{\psi DD\pi} = -ig_{\psi DD\pi} \varepsilon^{\mu\nu\alpha\beta} \psi_\mu \partial_\nu D \partial_\alpha \pi \partial_\beta \bar{D}, \quad (3c)$$

$$\mathcal{L}_{\psi D^* D^* \pi} = -ig_{\psi D^* D^* \pi} \varepsilon^{\mu\nu\alpha\beta} \psi_\mu D_\nu^* \partial_\alpha \pi \bar{D}_\beta^* - ih_{\psi D^* D^* \pi} \varepsilon^{\mu\nu\alpha\beta} \partial_\mu \psi_\nu D_\alpha^* \pi \bar{D}_\beta^*, \quad (3d)$$

$$\mathcal{L}_{D^* D \rho} = -g_{D^* D \rho} \varepsilon^{\mu\nu\alpha\beta} (D \partial_\mu \rho_\nu \partial_\alpha \bar{D}_\beta^* + \partial_\mu D_\nu^* \partial_\alpha \rho_\beta \bar{D}), \quad (3e)$$

$$\begin{aligned} \mathcal{L}_{\psi D^* D \rho} &= ig_{\psi D^* D \rho} \varepsilon^{\mu\nu\alpha\beta} \psi_\mu (\partial_\nu D \rho_\alpha \bar{D}_\beta^* + D_\nu^* \rho_\alpha \partial_\beta \bar{D}) \\ &\quad - ih_{\psi D^* D \rho} \varepsilon^{\mu\nu\alpha\beta} \psi_\mu (D \rho_\nu \partial_\alpha \bar{D}_\beta^* - \partial_\nu D_\alpha^* \rho_\beta \bar{D}), \end{aligned} \quad (3f)$$

with $\varepsilon_{0123} = +1$. In the heavy mass limit, due to the heavy quark spin symmetry, the pseudoscalars and vectors become degenerate and have to be treated on the same footing. As a consequence, the anomalous $D^* D^* \pi$ interaction term is required and can be related to the $D^* D \pi$ interaction term by the heavy quark spin symmetry [20,21].

Let us first evaluate the absorption processes of the J/ψ by π and ρ mesons within the effective Lagrangian obtained above. The values of the coupling constants will be discussed later. In this study, we assume that the J/ψ is a pure $\bar{c}c$ state and consider the OZI-preserving processes only at the tree level. The diagrams we are calculating are shown in Figs. 1 and 2. Compared to the previous studies [16,17], we find that the anomalous parity interactions open new absorption channels, namely $\pi + J/\psi \rightarrow D + \bar{D}$ [Diagram (1)], $\pi + J/\psi \rightarrow D^* + \bar{D}^*$ [Diagram (3)], and $\rho + J/\psi \rightarrow D^* + \bar{D}$ [Diagram (5)]. These processes are not allowed by the normal terms and were not considered before in the effective Lagrangian approach. In the quark exchange model [13,14], however, the processes $\pi + J/\psi \rightarrow D^* + \bar{D}^*$ and $\rho + J/\psi \rightarrow D^* + \bar{D}$ were calculated. There, $\pi + J/\psi \rightarrow D + \bar{D}$ was not considered since the absorption amplitude vanishes unless one considers the spin-orbit force [14,30]. A recent study using the Dyson-Schwinger formalism shows that the cross section for $\pi + J/\psi \rightarrow D + \bar{D}$ is small [30]. The anomalous terms also allow new absorption mechanisms to the previously considered absorption channels. These are Diagrams (2b), (4c), (4d), (6a), and (6b) of Figs. 1 and 2. As we shall see, the role of those diagrams is not negligible especially for the J/ψ absorption by the π 's.

We first calculate the absorption amplitude of $\pi + J/\psi$. We define the four-momenta of the J/ψ and π by p_1 and p_2 , respectively. We also denote the four-momenta of the final particles by p_3 and p_4 , which then defines $s = (p_1 + p_2)^2$ and $t = (p_1 - p_3)^2$. The polarization vector of the vector meson with momentum p_i is represented by ε_i . M_D and M_{D^*} represent the D and D^* meson masses, respectively. Then the differential cross section for this process is

$$\frac{d\sigma}{dt} = \frac{1}{96\pi s \mathbf{p}_1^2} \sum_{\text{spin}} |\mathcal{M}|^2, \quad (4)$$

where \mathbf{p}_1 is the three-momentum of p_1 in the center of mass frame. Note that we have multiplied factor 2 to get Eq. (4). This comes from summing over the possible isospin quantum numbers of the final state [17]. In computing Diagram (1) in Fig. 1, the four-momenta of the D and \bar{D} are represented by p_3 and p_4 , respectively. The absorption amplitude for this diagram can be written as

$$\mathcal{M} = \sum_i \mathcal{M}_\mu^{(1i)} \varepsilon_1^\mu, \quad (5)$$

where

$$\begin{aligned}
\mathcal{M}_\mu^{(1a)} &= -\frac{g_{D^*D\pi}g_{\psi D^*D}}{(p_2-p_3)^2-M_{D^*}^2}\varepsilon_{\mu\beta\lambda\rho}\left\{g^{\alpha\beta}-\frac{(p_2-p_3)^\alpha(p_2-p_3)^\beta}{M_{D^*}^2}\right\}p_{2\alpha}p_1^\lambda p_4^\rho, \\
\mathcal{M}_\mu^{(1b)} &= -\frac{g_{D^*D\pi}g_{\psi D^*D}}{(p_1-p_3)^2-M_{D^*}^2}\varepsilon_{\mu\beta\lambda\rho}\left\{g^{\alpha\beta}-\frac{(p_1-p_3)^\alpha(p_1-p_3)^\beta}{M_{D^*}^2}\right\}p_{2\alpha}p_1^\lambda p_3^\rho, \\
\mathcal{M}_\mu^{(1c)} &= g_{\psi DD\pi}\varepsilon_{\mu\beta\lambda\rho}p_2^\beta p_3^\lambda p_4^\rho.
\end{aligned} \tag{6}$$

In Diagram (2) of Fig. 1, the four-momenta of the D^* and \bar{D} are denoted by p_3 and p_4 , respectively, and we have

$$\mathcal{M} = \varepsilon_3^{*\nu} \sum_i \mathcal{M}_{\mu\nu}^{(2i)} \varepsilon_1^\mu, \tag{7}$$

where

$$\begin{aligned}
\mathcal{M}_{\mu\nu}^{(2a)} &= \frac{2g_{D^*D\pi}g_{\psi DD}}{(p_2-p_3)^2-M_D^2}p_{2\nu}p_{4\mu}, \\
\mathcal{M}_{\mu\nu}^{(2b)} &= -\frac{g_{D^*D^*\pi}g_{\psi D^*D}}{(p_2-p_3)^2-M_{D^*}^2}\varepsilon_{\mu\gamma\delta\beta}\varepsilon_{\nu\lambda\rho\alpha}\left\{g^{\alpha\beta}-\frac{(p_2-p_3)^\alpha(p_2-p_3)^\beta}{M_{D^*}^2}\right\}p_1^\gamma p_2^\rho p_3^\lambda p_4^\delta, \\
\mathcal{M}_{\mu\nu}^{(2c)} &= -\frac{1}{2}\frac{g_{D^*D\pi}g_{\psi D^*D^*}}{(p_1-p_3)^2-M_{D^*}^2}\left\{g^{\alpha\beta}-\frac{(p_1-p_3)^\alpha(p_1-p_3)^\beta}{M_{D^*}^2}\right\} \\
&\quad \times (p_{2\alpha}+p_{4\alpha})[2p_{3\mu}g_{\nu\beta}-(p_1+p_3)_\beta g_{\mu\nu}+2p_{1\nu}g_{\mu\beta}], \\
\mathcal{M}_{\mu\nu}^{(2d)} &= -g_{\psi D^*D\pi}g_{\mu\nu}.
\end{aligned} \tag{8}$$

For Diagram (3) of Fig. 1, we write the four-momenta of the D^* and \bar{D}^* by p_3 and p_4 , respectively, and we have

$$\mathcal{M} = \varepsilon_4^{*\lambda} \varepsilon_3^{*\nu} \sum_i \mathcal{M}_{\mu\nu\lambda}^{(3i)} \varepsilon_1^\mu, \tag{9}$$

where

$$\begin{aligned}
\mathcal{M}_{\mu\nu\lambda}^{(3a)} &= \frac{g_{D^*D\pi}g_{\psi D^*D}}{(p_2-p_3)^2-M_D^2}\varepsilon_{\mu\lambda\gamma\delta}p_1^\gamma p_{2\nu}p_4^\delta, \\
\mathcal{M}_{\mu\nu\lambda}^{(3b)} &= -\frac{g_{D^*D\pi}g_{\psi D^*D}}{(p_1-p_3)^2-M_D^2}\varepsilon_{\mu\nu\gamma\delta}p_1^\gamma p_{2\lambda}p_3^\delta, \\
\mathcal{M}_{\mu\nu\lambda}^{(3c)} &= -\frac{g_{D^*D^*\pi}g_{\psi D^*D^*}}{(p_2-p_3)^2-M_{D^*}^2}\left\{g^{\alpha\beta}-\frac{(p_2-p_3)^\alpha(p_2-p_3)^\beta}{M_{D^*}^2}\right\} \\
&\quad \times \varepsilon_{\nu\gamma\delta\alpha}p_3^\gamma p_2^\delta [2p_{4\mu}g_{\beta\lambda}-(p_1+p_4)_\beta g_{\mu\lambda}+2p_{1\lambda}g_{\mu\beta}], \\
\mathcal{M}_{\mu\nu\lambda}^{(3d)} &= -\frac{g_{D^*D^*\pi}g_{\psi D^*D^*}}{(p_1-p_3)^2-M_{D^*}^2}\left\{g^{\alpha\beta}-\frac{(p_1-p_3)^\alpha(p_1-p_3)^\beta}{M_{D^*}^2}\right\} \\
&\quad \times \varepsilon_{\lambda\gamma\delta\alpha}p_2^\gamma p_4^\delta [2p_{3\mu}g_{\beta\nu}-(p_1+p_3)_\beta g_{\mu\nu}+2p_{1\nu}g_{\mu\beta}], \\
\mathcal{M}_{\mu\nu\lambda}^{(3e)} &= -g_{\psi D^*D^*\pi}\varepsilon_{\mu\nu\lambda\rho}p_2^\rho - h_{\psi D^*D^*\pi}\varepsilon_{\mu\nu\lambda\rho}p_1^\rho.
\end{aligned} \tag{10}$$

We now calculate the J/ψ absorption by the ρ meson as shown in Fig. 2. We first define the four-momenta of the J/ψ and ρ as p_1 and p_2 respectively. Then the differential cross section reads

$$\frac{d\sigma}{dt} = \frac{1}{288\pi s p_1^2} \sum_{\text{spin}} |\mathcal{M}|^2. \quad (11)$$

For Diagram (4) of Fig. 2, we define p_3 and p_4 as the four-momenta of D and \bar{D} respectively. Then,

$$\mathcal{M} = \sum_i \mathcal{M}_{\mu\nu}^{(4i)} \varepsilon_1^\mu \varepsilon_2^\nu, \quad (12)$$

where

$$\begin{aligned} \mathcal{M}_{\mu\nu}^{(4a)} &= \frac{4g_{DD\rho}g_{\psi DD}}{(p_2 - p_3)^2 - M_D^2} p_{3\nu} p_{4\mu}, \\ \mathcal{M}_{\mu\nu}^{(4b)} &= \frac{4g_{DD\rho}g_{\psi DD}}{(p_1 - p_3)^2 - M_D^2} p_{4\nu} p_{3\mu}, \\ \mathcal{M}_{\mu\nu}^{(4c)} &= -\frac{g_{D^*D\rho}g_{\psi D^*D}}{(p_2 - p_3)^2 - M_{D^*}^2} \left\{ g^{\alpha\beta} - \frac{(p_2 - p_3)^\alpha (p_2 - p_3)^\beta}{M_{D^*}^2} \right\} \varepsilon_{\nu\gamma\delta\alpha} \varepsilon_{\mu\lambda\rho\beta} p_1^\lambda p_2^\gamma p_3^\delta p_4^\rho, \\ \mathcal{M}_{\mu\nu}^{(4d)} &= \frac{g_{D^*D\rho}g_{\psi D^*D}}{(p_1 - p_3)^2 - M_{D^*}^2} \left\{ g^{\alpha\beta} - \frac{(p_1 - p_3)^\alpha (p_1 - p_3)^\beta}{M_{D^*}^2} \right\} \varepsilon_{\nu\gamma\delta\alpha} \varepsilon_{\mu\lambda\rho\beta} p_1^\lambda p_2^\delta p_3^\rho p_4^\gamma, \\ \mathcal{M}_{\mu\nu}^{(4e)} &= g_{\psi DD\rho} g_{\mu\nu}. \end{aligned} \quad (13)$$

For Diagram (5) of Fig. 2, p_3 and p_4 are defined to be the four-momenta of the D^* and \bar{D} respectively. We have

$$\mathcal{M} = \varepsilon_3^{*\lambda} \sum_i \mathcal{M}_{\mu\nu\lambda}^{(5i)} \varepsilon_1^\mu \varepsilon_2^\nu, \quad (14)$$

where

$$\begin{aligned} \mathcal{M}_{\mu\nu\lambda}^{(5a)} &= -\frac{2g_{D^*D\rho}g_{\psi DD}}{(p_2 - p_3)^2 - M_D^2} \varepsilon_{\nu\lambda\gamma\delta} p_2^\delta p_3^\gamma p_{4\mu}, \\ \mathcal{M}_{\mu\nu\lambda}^{(5b)} &= \frac{2g_{DD\rho}g_{\psi D^*D}}{(p_1 - p_3)^2 - M_D^2} \varepsilon_{\lambda\mu\gamma\delta} p_1^\gamma p_3^\delta p_{4\nu}, \\ \mathcal{M}_{\mu\nu\lambda}^{(5c)} &= -\frac{g_{D^*D\rho}g_{\psi D^*D}}{(p_2 - p_3)^2 - M_{D^*}^2} \left\{ g^{\alpha\beta} - \frac{(p_2 - p_3)^\alpha (p_2 - p_3)^\beta}{M_{D^*}^2} \right\} \\ &\quad \times \varepsilon_{\mu\gamma\delta\beta} p_1^\gamma p_4^\delta [2p_{3\nu} g_{\lambda\alpha} - (p_2 + p_3)_\alpha g_{\nu\lambda} + 2p_{2\lambda} g_{\nu\alpha}], \\ \mathcal{M}_{\mu\nu\lambda}^{(5d)} &= -\frac{g_{D^*D\rho}g_{\psi D^*D}}{(p_1 - p_3)^2 - M_{D^*}^2} \left\{ g^{\alpha\beta} - \frac{(p_1 - p_3)^\alpha (p_1 - p_3)^\beta}{M_{D^*}^2} \right\} \\ &\quad \times \varepsilon_{\nu\gamma\delta\alpha} p_2^\delta p_4^\gamma [2p_{3\mu} g_{\beta\lambda} - (p_1 + p_3)_\beta g_{\mu\lambda} + 2p_{1\lambda} g_{\mu\beta}], \\ \mathcal{M}_{\mu\nu\lambda}^{(5e)} &= -g_{\psi D^*D\rho} \varepsilon_{\mu\nu\lambda\delta} p_4^\delta + h_{\psi D^*D\rho} \varepsilon_{\mu\nu\lambda\delta} p_3^\delta. \end{aligned} \quad (15)$$

Finally for Diagram (6) of Fig. 2, we denote the four-momenta of the D^* and \bar{D}^* by p_3 and p_4 , respectively, then we have

$$\mathcal{M} = \varepsilon_4^{*\rho} \varepsilon_3^{*\lambda} \sum_i \mathcal{M}_{\mu\nu\lambda\rho}^{(6i)} \varepsilon_1^\mu \varepsilon_2^\nu, \quad (16)$$

and

$$\begin{aligned}
\mathcal{M}_{\mu\nu\lambda\rho}^{(6a)} &= -\frac{g_{D^*D\rho}g_{\psi D^*D}}{(p_2-p_3)^2-M_D^2}\varepsilon_{\nu\lambda\gamma\delta}\varepsilon_{\mu\rho\alpha\beta}p_1^\alpha p_2^\delta p_3^\gamma p_4^\beta, \\
\mathcal{M}_{\mu\nu\lambda\rho}^{(6b)} &= \frac{g_{D^*D\rho}g_{\psi D^*D}}{(p_1-p_3)^2-M_D^2}\varepsilon_{\nu\rho\gamma\delta}\varepsilon_{\mu\lambda\alpha\beta}p_1^\alpha p_2^\gamma p_3^\beta p_4^\delta, \\
\mathcal{M}_{\mu\nu\lambda\rho}^{(6c)} &= -\frac{g_{D^*D^*\rho}g_{\psi D^*D^*}}{(p_2-p_3)^2-M_{D^*}^2}\left\{g^{\alpha\beta}-\frac{(p_2-p_3)^\alpha(p_2-p_3)^\beta}{M_{D^*}^2}\right\} \\
&\quad \times [2p_{3\nu}g_{\alpha\lambda}-(p_2+p_3)_\alpha g_{\nu\lambda}+2p_{2\lambda}g_{\nu\alpha}][2p_{4\mu}g_{\beta\rho}-(p_1+p_4)_\beta g_{\mu\rho}+2p_{1\rho}g_{\mu\beta}], \\
\mathcal{M}_{\mu\nu\lambda\rho}^{(6d)} &= -\frac{g_{D^*D^*\rho}g_{\psi D^*D^*}}{(p_1-p_3)^2-M_{D^*}^2}\left\{g^{\alpha\beta}-\frac{(p_1-p_3)^\alpha(p_1-p_3)^\beta}{M_{D^*}^2}\right\} \\
&\quad \times [2p_{4\nu}g_{\alpha\rho}-(p_2+p_4)_\alpha g_{\nu\rho}+2p_{2\rho}g_{\nu\alpha}][2p_{3\mu}g_{\beta\lambda}-(p_1+p_3)_\beta g_{\mu\lambda}+2p_{1\lambda}g_{\mu\beta}], \\
\mathcal{M}_{\mu\nu\lambda\rho}^{(6e)} &= -g_{\psi D^*D^*\rho}(2g_{\mu\nu}g_{\lambda\rho}-g_{\mu\rho}g_{\nu\lambda}-g_{\mu\lambda}g_{\nu\rho}). \tag{17}
\end{aligned}$$

In writing the above amplitudes, we have used $p_i \cdot \varepsilon_i = 0$. Note that the cross section for $\pi(\rho) + J/\psi \rightarrow D + \bar{D}^*$ is the same as that of $\pi(\rho) + J/\psi \rightarrow D^* + \bar{D}$.

III. COUPLING CONSTANTS AND CROSS SECTIONS

A. Coupling constants

To estimate the cross sections, let us first determine the coupling constants of our effective Lagrangian (1) and (3). We follow the methods of Refs. [16,17] to determine the couplings for the normal interactions. Here we briefly explain the method referring to Refs. [16,17] for details. The coupling constant of $D^*D\pi$ can be determined from the experimental data of $D^* \rightarrow D\pi$ decay. Our effective Lagrangian gives

$$\Gamma_{D^* \rightarrow D\pi} = \frac{g_{D^*D\pi}^2 |\mathbf{P}_\pi|^3}{24\pi M_{D^*}^2}. \tag{18}$$

However, at present, only its upper bound ($\simeq 0.131$ MeV) is known experimentally [31,32], which translates into $g_{D^*D\pi} \leq 14.7$. Therefore, we can only rely on model predictions such as those based on the QCD sum rule approach [33] or relativistic quark potential model [34]. Here we will take the value obtained in Ref. [33] and use²

$$g_{D^*D\pi} = 8.8. \tag{19}$$

For ψDD , $DD\rho$ and ψD^*D^* , $D^*D^*\rho$ couplings, we will follow Refs. [15,17] and make use of the vector meson dominance model (VDM). By applying VDM to the couplings of γD^+D^- and $\gamma D^0\bar{D}^0$, one obtains [17]

²Note that our convention is different from that of Ref. [33] by a factor of $\sqrt{2}$.

$$g_{\psi DD} = \frac{2}{3}g_{J/\psi} = 7.71, \quad g_{DD\rho} = \frac{1}{2}g_{\rho} = 2.52, \quad (20)$$

where g_V is determined from

$$\Gamma_{V \rightarrow e^+e^-} = \frac{4\pi\alpha_{\text{em}}^2 M_V}{3 g_V^2}, \quad (21)$$

with the vector meson mass M_V and $\alpha_{\text{em}} = e^2/4\pi$. The same method can be applied to the couplings of $\gamma D^{*+} D^{*-}$ and $\gamma D^{*0} \bar{D}^{*0}$. This gives

$$g_{\psi D^* D^*} = g_{\psi DD}, \quad g_{D^* D^* \rho} = g_{DD\rho}. \quad (22)$$

It is shown in Ref. [17] that the SU(4) symmetry values are not far from the above estimates except $g_{\psi DD}$.

There is no experimental or phenomenological informations on the 4-point vertices. Hence, we will rely on the SU(4) symmetry relations. Following Ref. [17], therefore, we assume that the appropriate symmetry breaking effects in the 4-point coupling constants are encoded via their relations to the 3-point vertices within SU(4) symmetry. Hence, using the phenomenological estimate of the 3-point vertices fixed above, we have

$$\begin{aligned} g_{\psi D^* D^* \pi} &= \frac{1}{2}g_{\psi DD}g_{D^* D^* \pi} \approx 33.92, \\ g_{\psi DD\rho} &= 2g_{\psi DD}g_{DD\rho} \approx 38.86, \\ g_{\psi D^* D^* \rho} &= g_{\psi D^* D^*}g_{D^* D^* \rho} \approx 19.43. \end{aligned} \quad (23)$$

We determine the couplings of the anomalous interactions in a similar way. As discussed before, the $D^* D^* \pi$ coupling is constrained by the heavy quark spin symmetry. Comparing with the effective Lagrangian of Ref. [24], we get to leading order in $1/\bar{M}(D)$

$$g_{D^* D^* \pi} = \frac{\bar{M}(D)}{2}g_{D^* D^* \pi} \approx 9.08 \text{ GeV}^{-1}, \quad (24)$$

where $\bar{M}(D)$ is the average mass of D and D^* .

For $\psi D^* D$ and $D^* D\rho$ couplings, we can apply VDM to the radiative decays of D^* into D , i.e., $D^* \rightarrow D\gamma$. Then by using the same technique explained before, we obtain

$$\begin{aligned} g_{\psi D^* D} &= \frac{2}{3}g_{J/\psi}g_V^{\pm} = \frac{2}{3}g_{J/\psi}g_V^0, \\ g_{D^* D\rho} &= \frac{1}{6}g_{\rho} (g_V^{\pm} + 2g_V^0), \end{aligned} \quad (25)$$

where $g_V^{\pm,0}$ are defined through

$$\begin{aligned} \langle D^+(k) | J_{\mu}^{em} | D^{*+}(p, \varepsilon) \rangle &= e g_V^{\pm} \varepsilon_{\mu\nu\alpha\beta} \varepsilon^{\nu} k^{\alpha} p^{\beta}, \\ \langle \bar{D}^0(k) | J_{\mu}^{em} | \bar{D}^{*0}(p, \varepsilon) \rangle &= e g_V^0 \varepsilon_{\mu\nu\alpha\beta} \varepsilon^{\nu} k^{\alpha} p^{\beta}. \end{aligned} \quad (26)$$

Then from the experimental values for the D^* radiative decays, we can determine the above coupling constants. However, at present, only an experimental upper bound is known for

the D^* decays. Therefore, we will use model prediction based on relativistic potential model given in Ref. [34], which gives

$$g_V = \frac{e_Q}{\Lambda_Q} + \frac{e_q}{\Lambda_q}, \quad (27)$$

where e_Q is the heavy quark charge and e_q the light quark charge with $\Lambda_Q = 1.57$ and $\Lambda_q = 0.48$ in GeV unit. This gives

$$g_V^\pm \approx 1.12 \text{ GeV}^{-1}, \quad g_V^0 \approx 0.96 \text{ GeV}^{-1}, \quad (28)$$

which then leads to

$$g_{\psi D^* D} = 7.40 \sim 8.64 \text{ GeV}^{-1}, \quad g_{D^* D \rho} = 2.82 \text{ GeV}^{-1}. \quad (29)$$

For the 4-point couplings, we depend on the SU(4) relations again, which gives

$$\begin{aligned} g_{\psi D^* D^* \pi} &= h_{\psi D^* D^* \pi} = \frac{1}{2} g_{\psi D^* D} g_{D^* D \pi} \approx 38.19 \text{ GeV}^{-1}, \\ g_{\psi D^* D \rho} &= h_{\psi D^* D \rho} = g_{\psi D^* D} g_{D^* D \rho} \approx 21.77 \text{ GeV}^{-1}. \end{aligned} \quad (30)$$

However, for the $\psi DD\pi$ coupling, it is not easy to write it in terms of the other 3-point coupling constants as can be seen from the difference in dimensions. Thus we directly use the SU(4) relation and assume that the symmetry breaking effects change F_π to F_D [35];

$$g_{\psi DD\pi} = \frac{g_{D^* D \pi} N_c}{6\pi^2 F_D^3} \approx 16.0 \text{ GeV}^{-3}. \quad (31)$$

Here we have used $F_D \approx 2.3F_\pi$ [32]. This completes the determination of our coupling constants. The values of the coupling constants are listed in Table I together with their fixing procedure.

B. Cross sections without form factors

We first give the cross sections for the J/ψ absorption processes without any form factors. Since our meson exchange model is not expected to work at high energies, we focus on the energy region near threshold in this paper. In Fig. 3 we show the cross sections for the J/ψ absorption processes obtained from Figs. 1 and 2. Although the $\pi + J/\psi \rightarrow D + \bar{D}$ process has the lowest threshold energy, its cross section (dotted line in the upper panel of Fig. 3) is suppressed compared to the other channels over the whole energy region. Nevertheless, this process was not considered previously in the meson exchange models. When the energy is less than the $D^* + \bar{D}$ threshold, this process alone is allowed, but the magnitude is very small and less than 0.1 mb. This observation is consistent with Ref. [30], although its energy dependence is different.

The $\pi + J/\psi \rightarrow D + \bar{D}^*$ has the same cross section as the $\pi + J/\psi \rightarrow D^* + \bar{D}$, and their sum is given by the dashed line in the upper panel of Fig. 3. These processes dominate for the energies from their threshold up to the $D^* + \bar{D}^*$ threshold. At higher energies, the

$\pi + J/\psi \rightarrow D^* + \bar{D}^*$ process dominates the absorption. Since the $D^* + \bar{D}^*$ threshold is larger than 4 GeV, the $\pi + J/\psi \rightarrow D^* + \bar{D}, D + \bar{D}^*$ is the dominant process for $\sqrt{s} \leq 4$ GeV.

The cross section for $\pi + J/\psi \rightarrow D^* + \bar{D}^*$ process (the dot-dashed line in the upper panel of Fig. 3) is the dominant one at large energies, which is in contrast to the quark exchange model calculations [13,14]. In addition to the effects from the form factors, this may indicate that the meson exchange approach for this reaction has non-trivial contributions from the exchanges of meson resonance with heavier mass, such as the D_1 exchange, because of its higher threshold. This process is allowed by the anomalous terms and was not considered in the previous meson exchange model studies.

In the lower panel of Fig. 3 we show the cross sections for the $\rho + J/\psi$ processes. It is shown that at very low energy, the exothermic $\rho + J/\psi \rightarrow D + \bar{D}$ is the dominant process (the dotted line in the lower panel of Fig. 3). But it is rapidly taken over by $\rho + J/\psi \rightarrow D^* + \bar{D}, D + \bar{D}^*$ process (the dashed line in the lower panel of Fig. 3), which also dominates at higher energies. This reaction is an anomalous parity process and was not studied before in the meson exchange model. The $\rho + J/\psi \rightarrow D^* + \bar{D}^*$ cross section (the dot-dashed line in the lower panel of Fig. 3) has a peak near threshold but has comparable size with that of $\rho + J/\psi \rightarrow D^* + \bar{D}, D + \bar{D}^*$.

The dashed lines in Fig. 4 show the results obtained with the normal terms only and are consistent with the results of Refs. [16–18]. The solid lines are the predictions of the full calculation including the anomalous terms. It is evident that the anomalous terms give non-trivial effects to the cross sections especially for the $\pi + J/\psi$ reaction. For comparison, we also calculate the normal processes considered in previous studies but with the additional diagrams with anomalous vertices. The results are given by the dot-dashed lines in Fig. 4. The difference between the dashed lines and dot-dashed lines are due to the anomalous processes, i.e., for $\pi + J/\psi \rightarrow D^* + \bar{D}, D + \bar{D}^*$ in the upper panel and for $\rho + J/\psi \rightarrow D + \bar{D}, D^* + \bar{D}^*$ in the lower panel. At low energy, i.e., $\sqrt{s} \leq 4$ GeV which corresponds to $E_{\text{kin}} = \sqrt{s} - M_{J/\psi} - M_\pi \leq 0.8$ GeV, where $M_{J/\psi}$ and M_π are the J/ψ and pion masses respectively, the anomalous interactions reduce the total absorption cross section for $\pi + J/\psi$ by about 50 %. Our numerical results show that the $\pi + J/\psi$ absorption cross section is less than 10 mb in this energy region. However, the contribution of the anomalous terms to the $\rho + J/\psi$ cross sections is not so important except at the high energy region, which is thought to have many corrections from higher meson resonances exchanges.

In Figs. 5 and 6, we show the contributions from each diagram for each channel. For $\pi + J/\psi \rightarrow D + \bar{D}$ and $\pi + J/\psi \rightarrow D^* + \bar{D}^*$, it can be seen that the contact diagrams (1c) and (3e) are important. However, considering the uncertainty related to the 4-point vertices, the results for this process are more qualitative. The more important and less uncertain process is the $\pi + J/\psi \rightarrow D^* + \bar{D}$. The interesting observation here is that the role of the anomalous term [(2b) of Fig. 1] is quite non-trivial at low energies and even dominates at higher energies. The strong interference with the normal terms leads to the substantial difference in the cross section as shown in the upper panel of Fig. 4. But in contrast, as can be seen from Fig. 6, the role of the anomalous terms in the $\rho + J/\psi$ absorption is not so crucial except $\rho + J/\psi \rightarrow D^* + \bar{D}, D + \bar{D}^*$ which is allowed only by including the anomalous vertices. Its effect becomes important at higher energies and is small at $\sqrt{s} \leq 4$ GeV.

C. Cross sections with form factors

As pointed out by Ref. [14], the assumption of t -channel exchange of a heavy meson is hard to justify without including form factors. This is so because the range of heavy meson exchange is much smaller than the physical sizes of the initial hadrons. There are some approaches to include form factors in the J/ψ absorption processes and different form factors and cutoff parameters are employed [17,18,36], which, of course, cannot be justified *a priori*. Microscopic models such as quark potential models may give us a guide for the form factors. Here, we employ the simple form of the form factors employed in Ref. [17], which are

$$F_3 = \frac{\Lambda^2}{\Lambda^2 + r^2}, \quad F_4 = \frac{\Lambda^2}{\Lambda^2 + \bar{r}^2} \frac{\Lambda^2}{\Lambda^2 + \bar{r}^2}, \quad (32)$$

where $r^2 = (\mathbf{p}_1 - \mathbf{p}_3)^2$ or $(\mathbf{p}_2 - \mathbf{p}_3)^2$ and $\bar{r} = [(\mathbf{p}_1 - \mathbf{p}_3)^2 + (\mathbf{p}_2 - \mathbf{p}_3)^2]/2$. F_3 is the form factor for the 3-point vertices and F_4 for the 4-point vertices. The cutoff parameters should be chosen experimentally and may take different values for different vertices. However, because of the paucity of experimental information, we use the same value for all cutoff parameters as in the literature and investigate the dependence of the cross sections on the cutoff parameters.

In Fig. 7 we show a similar figure as in Fig. 4 but with the form factors of Eq. (32) with $\Lambda = 2$ GeV (left panel) and 1 GeV (right panel). It can be seen that the role of the form factors are more important at higher energy region and suppresses the overall cross sections. But the tendency shown in Fig. 4 is still valid, i.e., the anomalous terms reduce the cross sections for $\pi + J/\psi$ at low energies through interference with the normal terms. Finally, Fig. 7 then shows that the cross sections for $\pi + J/\psi$ absorption process is about $2 \sim 6$ mb depending on the cutoff parameter at $\sqrt{s} \leq 4$ GeV. The $\rho + J/\psi$ cross section is very small at $\sqrt{s} \leq 4$ GeV and has maximum value of $3 \sim 9$ mb for intermediate energies up to 5 GeV.

IV. SUMMARY AND DISCUSSIONS

Knowing the magnitude and energy dependence of the J/ψ absorption cross sections by hadrons is crucial to estimate the effect of J/ψ suppression in RHIC due to hadronic processes. We have re-examined the J/ψ absorption by π and ρ mesons in a meson exchange model. The absorption processes are dominated by the D and the D^* exchanges. By including anomalous parity interactions we found that additional channels and absorption mechanisms are allowed. Their contribution was found to be quite non-trivial especially for $\pi + J/\psi$ cross section. The calculated cross section for $\pi + J/\psi$ at low energies was found to be only about one half of the previous calculations [16–18]. With conventional, but arbitrarily chosen, form factors and cutoff parameters, the $\pi + J/\psi$ cross section was estimated to be $2 \sim 6$ mb for $\sqrt{s} \leq 4$ GeV. In contrast, the effect of anomalous terms was found to be weak in $\rho + J/\psi$ cross section at low energies.

In addition to the uncertainties related to the determination of the coupling constants and form factors, our model calculation may be improved further. One such improvement would be the inclusion of the axial-vector $D_1(2420)$ meson exchanges, as mentioned in Ref.

[16]. Also at low energy, final state interactions are expected to improve the calculation. It would be also interesting to investigate other possible absorption channels as in Ref. [18]. For example, one may consider OZI-evading vertices such as the J/ψ - ρ - π coupling, which can allow new absorption channels with much smaller thresholds than the processes considered in this work, although such processes are expected to be suppressed.

ACKNOWLEDGMENTS

We are grateful to C.-Y. Wong for fruitful discussions and encouragement. This work was supported in part by the Brain Korea 21 project of Korean Ministry of Education and by KOSEF under Grant No. 1999-2-111-005-5.

APPENDIX:

In this Appendix we briefly explain the way to obtain the effective Lagrangian (1) and (3). As in the literature [15–18] we start with the SU(4) symmetric chiral Yang-Mills Lagrangian [27],

$$\begin{aligned} \mathcal{L}_{\chi YM} = & \frac{F_\pi^2}{8} \text{Tr} (D_\mu U D^\mu U^\dagger) + \frac{F_\pi^2}{8} \text{Tr} [M (U + U^\dagger - 2)] \\ & - \frac{1}{2} \text{Tr} (F_{\mu\nu}^L F^{L\mu\nu} + F_{\mu\nu}^R F^{R\mu\nu}) + m_0^2 (A_\mu^L A^{L\mu} + A_\mu^R A^{R\mu}), \end{aligned} \quad (\text{A1})$$

where $U = \exp(i2\phi/F_\pi)$ with the pion decay constant F_π (≈ 132 MeV) and $\phi = \pi^a \lambda^a / \sqrt{2}$. The covariant derivative is defined as

$$D_\mu U = \partial_\mu U - ig A_\mu^L U + ig U A_\mu^R, \quad (\text{A2})$$

with left- and right-handed spin-1 fields $A_\mu^{L,R}$, which are related to the vector and axial-vector mesons V_μ ($= V_\mu^a \lambda^a / \sqrt{2}$) and A_μ ($= A_\mu^a \lambda^a / \sqrt{2}$) by

$$A_{L\mu} = \frac{1}{2} (V_\mu + A_\mu), \quad A_{R\mu} = \frac{1}{2} (V_\mu - A_\mu). \quad (\text{A3})$$

The field strength tensors are

$$F_{\mu\nu}^{L,R} = \partial_\mu A_\nu^{L,R} - \partial_\nu A_\mu^{L,R} - ig [A_\mu^{L,R}, A_\nu^{L,R}]. \quad (\text{A4})$$

In obtaining the Lagrangian (A1) we do not take any non-minimal terms into account for simplicity.

It is straightforward to obtain the interaction Lagrangian for ϕ and V , which leads to

$$\begin{aligned} \mathcal{L}_n^{VP} = & -\frac{ig}{2} \text{Tr} \{V_\mu (\phi \partial^\mu \phi - \partial^\mu \phi \phi)\} + \frac{ig}{4} \text{Tr} (\partial_\mu V_\nu - \partial_\nu V_\mu) [V^\mu, V^\nu] \\ & - \frac{g^2}{8} \text{Tr} [V_\mu, \phi] [V^\mu, \phi] + \frac{g^2}{16} \text{Tr} [V_\mu, V_\nu]^2, \end{aligned} \quad (\text{A5})$$

where we have ignored the A - ϕ mixing effects as they are of order of $1/M_V^2$. The above Lagrangian was obtained by keeping the axial-vector field. As in Ref. [28], one may gauge-out the axial-vector field. It is found that including proper non-minimal terms gives the same form for the effective Lagrangian as Eq. (A5) with different coupling constant [18], i.e., by substituting $2g$ for the coupling constant of Ref. [18] one can get the effective Lagrangian in the form of Eq. (A5).

The anomalous parity terms come from nine gauged Wess-Zumino terms, which read

$$\begin{aligned}
\mathcal{L}_{\text{an}} = & 5Ci \text{Tr} [A_L L^3 + A_R R^3] - 5C \text{Tr} [(dA_L A_L + A_L dA_L)L + (dA_R A_R + A_R dA_R)R] \\
& + 5C \text{Tr} [dA_L dU A_R U^\dagger - dA_R dU^\dagger A_L U] + 5C \text{Tr} [A_R U^\dagger A_L U R^2 - A_L U A_R U^\dagger L^2] \\
& + \frac{5C}{2} \text{Tr} [(A_L L)^2 - (A_R R)^2] + 5Ci \text{Tr} [A_L^3 L + A_R^3 R] \\
& + 5Ci \text{Tr} [(dA_R A_R + A_R dA_R) U^\dagger A_L U - (dA_L A_L + A_L dA_L) U A_R U^\dagger] \\
& + 5Ci \text{Tr} [A_L U A_R U^\dagger A_L L + A_R U^\dagger A_L U A_R R] \\
& + 5C \text{Tr} \left[A_R^3 U^\dagger A_L U - A_L^3 U A_R U + \frac{1}{2} (U A_R U^\dagger A_L)^2 \right], \tag{A6}
\end{aligned}$$

where $C = -iN_c/240\pi^2$ with the number of color N_c and $L = dUU^\dagger$, $R = U^\dagger dU$. We have used 1-form notation in writing the above Lagrangian.

For simplicity we again ignore the A - ϕ mixing and use the Bardeen subtracted form for the anomalous terms. This gives

$$\begin{aligned}
\mathcal{L}_{\text{an}}^{VP} = & -\frac{g^2 N_c}{16\pi^2 F_\pi} \text{Tr} (dV dV \phi) - \frac{ig N_c}{6\pi^2 F_\pi^3} \text{Tr} \{V(d\phi)^3\} \\
& + \frac{ig^3 N_c}{32\pi^2 F_\pi} \text{Tr} (V^3 d\phi) + \frac{ig^3 N_c}{32\pi^2 F_\pi} \text{Tr} (V dV V \phi). \tag{A7}
\end{aligned}$$

Writing the pseudoscalar and vector fields explicitly and assuming pure $\bar{c}c$ for the J/ψ wave function, we can obtain the effective Lagrangian (1) and (3) as well as the SU(4) symmetry relations used in Sec. III. Note that by eliminating the axial-vector fields, the coupling constant of $V\phi\phi\phi$ interaction becomes [28]

$$g_{V\phi\phi\phi} = \frac{M_V^2}{\pi^2 g_{V\phi\phi} F_\pi^5}. \tag{A8}$$

Assuming that the proper symmetry breaking terms make $M_V \rightarrow M_{D^*}$, $g_{V\phi\phi} \rightarrow g_{D^*D\pi}$, and $F_\pi \rightarrow F_D$ in the above relation, we get $g_{\psi DD\pi} \approx 18.0 \text{ GeV}^{-3}$, which is close to the value listed in Table I.

REFERENCES

- [1] T. Matsui and H. Satz, Phys. Lett. B **178**, 416 (1986).
- [2] H. Satz, Rep. Prog. Phys. **63**, 1511 (2000); Univ. Bielefeld Report No. BI-TP-2000/31, hep-ph/0009099.
- [3] NA50 Collaboration, M. Gonin *et al.*, Nucl. Phys. **A610**, 404c (1996).
- [4] NA50 Collaboration, M. C. Abreu *et al.*, Phys. Lett. B **477**, 28 (2000).
- [5] J.-P. Blaizot and J.-Y. Ollitrault, Phys. Rev. Lett. **77**, 1703 (1996).
- [6] C.-Y. Wong, Nucl. Phys. **A630**, 487c (1998); Talk at 3rd Catania Relativistic Ion Studies on Phase Transitions Strong Interactions: Status and Perspectives (CRIS 2000), Italy, May, 2000, nucl-th/0007046.
- [7] J. Ftáčnik, P. Lichard, and J. Pišút, Phys. Lett. B **207**, 194 (1988); S. Gavin, M. Gyulassy, and A. Jackson, *ibid.* **207**, 257 (1988); R. Vogt, M. Prakash, P. Koch, and T. H. Hansson, *ibid.* **207**, 263 (1988).
- [8] W. Cassing and C. M. Ko, Phys. Lett. B **396**, 39 (1997).
- [9] W. Cassing and E. L. Bratkovskaya, Nucl. Phys. **A623**, 570 (1997).
- [10] N. Armesto and A. Capella, Phys. Lett. B **430**, 23 (1998); A. Capella, E. G. Ferreira, and A. B. Kaidalov, Phys. Rev. Lett. **85**, 2080 (2000); A. Sibirtsev, K. Tsushima, K. Saito, and A. W. Thomas, Phys. Lett. B **484**, 23 (2000).
- [11] D. Kharzeev and H. Satz, Phys. Lett. B **334**, 155 (1994).
- [12] D. Kharzeev, H. Satz, A. Syamtomov, and G. Zinovjev, Phys. Lett. B **389**, 595 (1996).
- [13] K. Martins, D. Blaschke, and E. Quack, Phys. Rev. C **51**, 2723 (1995).
- [14] C.-Y. Wong, E. S. Swanson, and T. Barnes, Phys. Rev. C **62**, 045201 (2000).
- [15] S. G. Matinyan and B. Müller, Phys. Rev. C **58**, 2994 (1998).
- [16] K. L. Haglin, Phys. Rev. C **61**, 031902 (2000).
- [17] Z. Lin and C. M. Ko, Phys. Rev. C **62**, 034903 (2000).
- [18] K. L. Haglin and C. Gale, St. Cloud State Univ. Report (2000), nucl-th/0010017.
- [19] M. E. Peskin, Nucl. Phys. **B156**, 365 (1979); G. Bhanot and M. E. Peskin, *ibid.* **B156**, 391 (1979).
- [20] M. B. Wise, Phys. Rev. D **45**, 2188 (1992).
- [21] T.-M. Yan, H.-Y. Cheng, C.-Y. Cheung, G.-L. Lin, Y. C. Lin, and H.-L. Yu, Phys. Rev. D **46**, 1148 (1992), **55**, 5851(E) (1997).
- [22] M. B. Voloshin and M. A. Shifman, Yad. Fiz. **45**, 463 (1987), [Sov. J. Nucl. Phys. **45**, 292 (1987)]; *ibid.* **47**, 801 (1988), [Sov. J. Nucl. Phys. **47**, 511 (1988)].
- [23] N. Isgur and M. B. Wise, Phys. Lett. B **232**, 113 (1989); **237**, 527 (1990).
- [24] L.-H. Chan, Phys. Rev. D **55**, 5362 (1997).
- [25] M. Luke and A. V. Manohar, Phys. Lett. B **286**, 348 (1992); Y.-Q. Chen, *ibid.* **317**, 421 (1993); M. Finkemeier, H. Georgi, and M. McIrvin, Phys. Rev. D **55**, 6933 (1997).
- [26] D.-P. Min, Y. Oh, B.-Y. Park, and M. Rho, Int. J. Mod. Phys. E **4**, 47 (1995).
- [27] See, e.g., U.-G. Meissner, Phys. Rep. **161**, 213 (1988).
- [28] Ö. Kaymakçalan and J. Schechter, Phys. Rev. D **31**, 1109 (1985).
- [29] Ö. Kaymakçalan, S. Rajeev, and J. Schechter, Phys. Rev. D **30**, 594 (1984).
- [30] D. B. Blaschke, G. R. G. Bureau, M. A. Ivanov, Yu. L. Kalinovsky, and P. C. Tandy, Univ. Rostock Report No. MPG-VT-UR-201-00, hep-ph/0002047.
- [31] ACCMOR Collaboration, S. Barlag *et al.*, Phys. Lett. B **278**, 480 (1992).

- [32] Particle Data Group, D. E. Groom *et al.*, Eur. Phys. J. C **15**, 1 (2000).
- [33] V. M. Belyaev, V. M. Braun, A. Khodjamirian, and R. Rückl, Phys. Rev. D **51**, 6177 (1995).
- [34] P. Colangelo, F. De Fazio, and G. Nardulli, Phys. Lett. B **334**, 175 (1994).
- [35] G. Pari, B. Schwesinger, and H. Walliser, Phys. Lett. B **255**, 1 (1991); Y. Oh, D.-P. Min, M. Rho, and N. N. Scoccola, Nucl. Phys. **A534**, 493 (1991).
- [36] K. Haglin and C. Gale, in *Hirschegg 2000: Hadrons in Dense Matter*, edited by M. Buballa, W. Nörenberg, B.-J. Schaefer, and J. Wambach, (GSI, Darmstadt, 2000), nucl-th/0002029.

TABLES

coupling constant	method	value
$g_{D^*D\pi}$	$D^* \rightarrow D\pi$ and QCD sum rule	8.84 [33]
$g_{\psi DD}$	γDD coupling and VDM	7.71 [15]
$g_{DD\rho}$	γDD coupling and VDM	2.52 [15]
$g_{\psi D^*D^*}$	γD^*D^* coupling and VDM	7.71 [15,17]
$g_{D^*D^*\rho}$	γD^*D^* coupling and VDM	2.52 [15,17]
$g_{\psi D^*D\pi}$	SU(4) symmetry relation	33.92 [17]
$g_{\psi DD\rho}$	SU(4) symmetry relation	38.86 [17]
$g_{\psi D^*D^*\rho}$	SU(4) symmetry relation	19.43 [17]
$g_{D^*D^*\pi}$	heavy quark spin symmetry	9.08 GeV ⁻¹
$g_{\psi D^*D}$	$D^* \rightarrow D\gamma$, VDM, and quark model	8.64 GeV ⁻¹
$g_{D^*D\rho}$	$D^* \rightarrow D\gamma$, VDM, and quark model	2.82 GeV ⁻¹
$g_{\psi DD\pi}$	SU(4) symmetry relation	16.00 GeV ⁻³
$g_{\psi D^*D^*\pi}$	SU(4) symmetry relation	38.19 GeV ⁻¹
$h_{\psi D^*D^*\pi}$	SU(4) symmetry relation	38.19 GeV ⁻¹
$g_{\psi D^*D\rho}$	SU(4) symmetry relation	21.77 GeV ⁻¹
$h_{\psi D^*D\rho}$	SU(4) symmetry relation	21.77 GeV ⁻¹

TABLE I. Determination of the coupling constants.

FIGURES

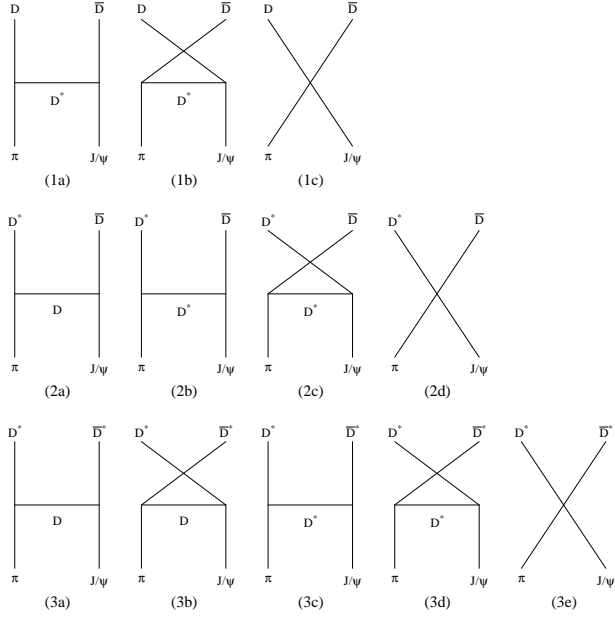


FIG. 1. Feynman diagrams for J/ψ absorption processes by pion: (1) $J/\psi + \pi \rightarrow D + \bar{D}$, (2) $J/\psi + \pi \rightarrow D^* + \bar{D}$, and (3) $J/\psi + \pi \rightarrow D^* + \bar{D}^*$. The process $J/\psi + \pi \rightarrow D + \bar{D}^*$ has the same cross section as (2).

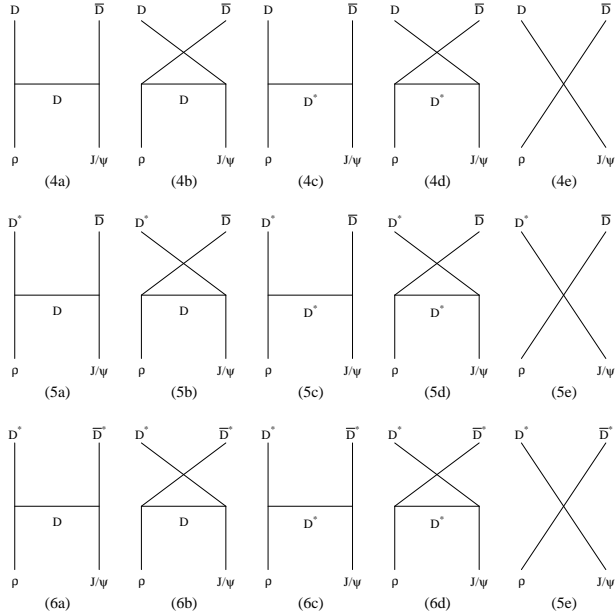


FIG. 2. Feynman diagrams for J/ψ absorption processes by ρ : (4) $J/\psi + \rho \rightarrow D + \bar{D}$, (5) $J/\psi + \rho \rightarrow D^* + \bar{D}$, and (6) $J/\psi + \rho \rightarrow D^* + \bar{D}^*$. The process $J/\psi + \rho \rightarrow D + \bar{D}^*$ has the same cross section as (5).

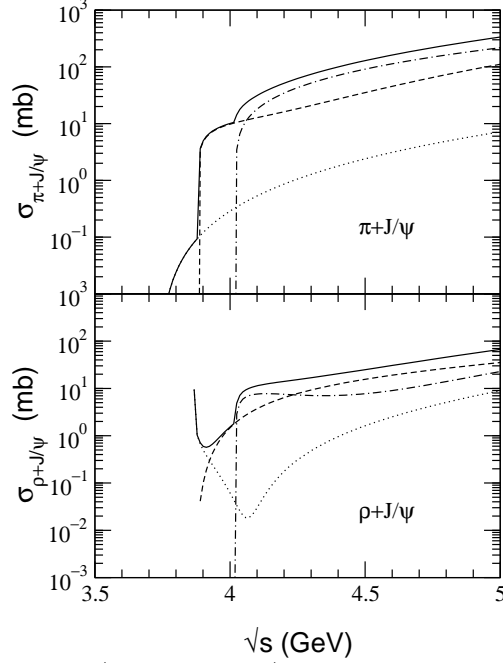


FIG. 3. Cross sections for $\pi + J/\psi$ and $\rho + J/\psi$. In the upper panel, the dotted, dashed, and dot-dashed lines correspond to Diagrams (1), (2), and (3), respectively. In the lower panel, the dotted, dashed, and dot-dashed lines correspond to Diagrams (4), (5), and (6), respectively. The solid lines are the sum of all processes.

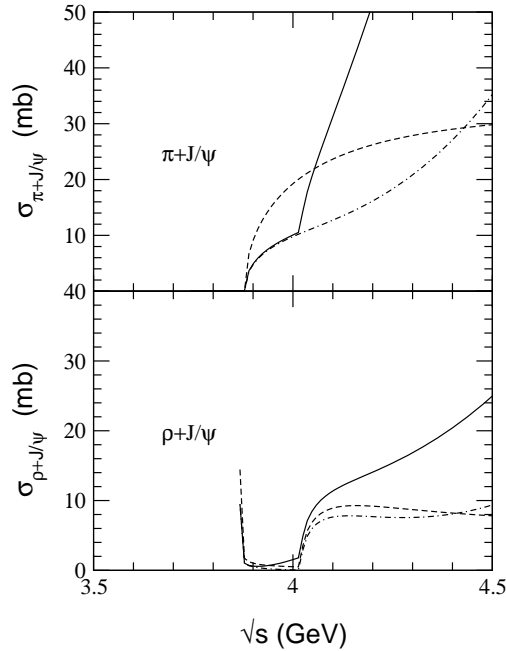


FIG. 4. Cross sections for $\pi + J/\psi$ and $\rho + J/\psi$. The solid lines are our model predictions and the dashed lines are those obtained without the anomalous terms. The dot-dashed lines correspond to $\pi + J/\psi \rightarrow D^* + \bar{D}, D + \bar{D}^*$ in the upper panel and $\rho + J/\psi \rightarrow D + \bar{D}, D^* + \bar{D}^*$ in the lower panel in full calculation.

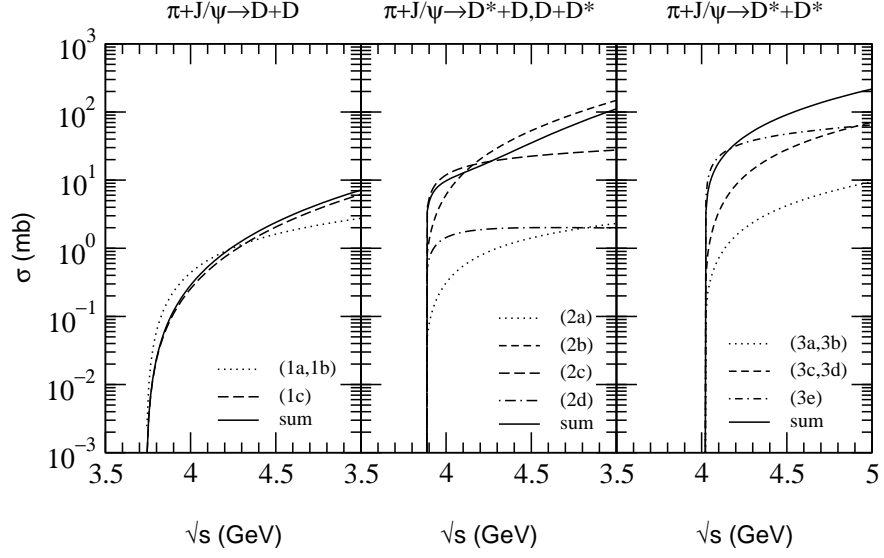


FIG. 5. Contributions from each diagram to the cross sections for $\pi + J/\psi$.

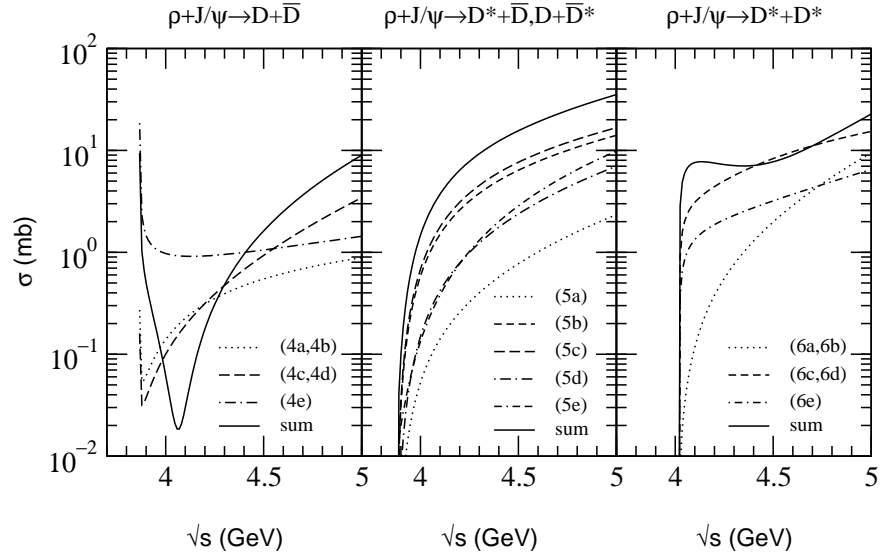


FIG. 6. Contributions from each diagram to the cross sections for $\rho + J/\psi$.

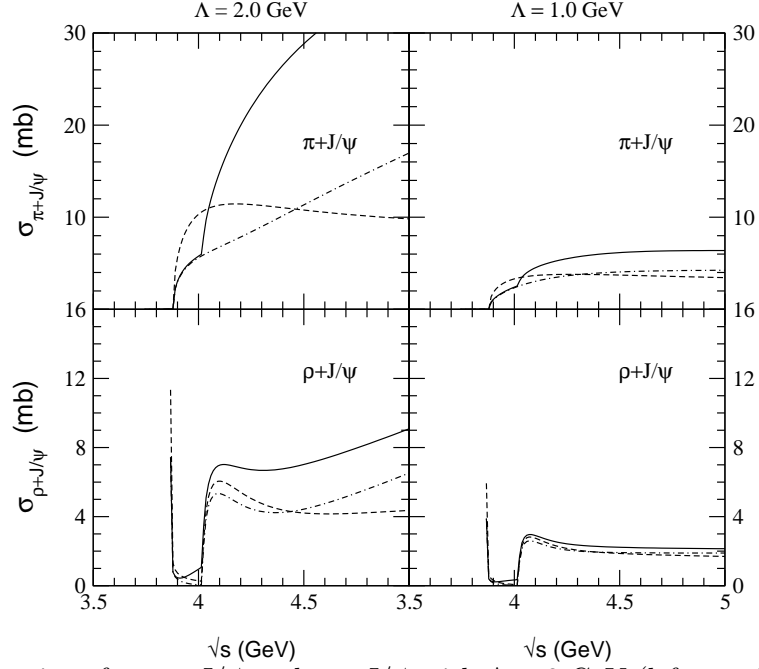


FIG. 7. Cross sections for $\pi + J/\psi$ and $\rho + J/\psi$ with $\Lambda = 2$ GeV (left panel) and 1 GeV (right panel). The notations are the same as in Fig. 4.